Airway Hyperresponsiveness, Remodeling, and Smooth Muscle Mass

Right Answer, Wrong Reason?

Madavi N. Oliver, Ben Fabry, Aleksandar Marinkovic, Srboljub M. Mijailovich, James P. Butler, and Jeffrey J. Fredberg

Physiology Program, Department of Environmental Health, Harvard School of Public Health, Boston, Massachusetts; and Department of Physics, Erlangen University, Erlangen, Germany

We quantified the effects of airway wall remodeling upon airway smooth muscle (ASM) shortening. Isolated ASM from sheep was attached to a servo-controller that applied a physiologic load. This load could be altered to reflect specified changes of airway wall geometry, elasticity, parenchymal tethering, transpulmonary pressure (P_L), and fluctuations in P_L associated with breathing. Starting at a reference length (L_{ref}), ASM was stimulated with acetylcholine and held at constant P_L of 4 cm H_2O for 2 h. When all compartments were thickened to simulate the asthmatic airway but P_L was held fixed, ASM shortened much more than that in the normal airway (to 0.52 L_{ref} versus 0.66 L_{ref}). When breathing with deep inspirations (DIs) was initiated, within the first three DIs the ASM in the normal airway lengthened to 0.84 L_{ref}, whereas that in the asthmatic airway remained stuck at 0.53 L_{ref}. Thickening of the smooth muscle layer alone produced the greatest muscle shortening (to 0.47 L_{ref}) when compared with thickening of only submucosal (to 0.67 L_{ref}) or only adventitial (to 0.62 L_{ref}) compartments. With increased ASM mass, the ASM failed to lengthen in response to DIs, whereas in the airway with thickened submucosal and adventitial layers ASM lengthened dramatically (to 0.83 L_{ref}). These findings confirm the long-held conclusion that increased muscle mass is the functionally dominant derangement, but mechanisms accounting for this conclusion differ dramatically from those previously presumed. Furthermore, increased ASM mass explained both hyperresponsiveness and the failure of a DI to relax the asthmatic airway.

Keywords: remodeling; asthma; hyperresponsiveness

Asthma is characterized by airways that constrict too easily (airway hypersensitivity) and too much (airway hyperresponsiveness, AHR) (1). It is the excessive airway narrowing associated with AHR, rather than the hypersensitivity, that accounts for the morbidity and the mortality that is attributable to the disease (2–4). AHR is thought to arise as a result of ongoing and irreversible remodeling of the airway wall (2, 5–10). Among the various factors that come into play, AHR might be accounted for either by increased mass of airway smooth muscle (ASM) or by decreased load against which the ASM must contract, but it is widely believed that increased ASM mass is the main culprit (11–13). This important conclusion is based mainly upon theoretical considerations, however, wherein structural evidence has been incorporated into detailed mathematical models of airway narrowing (11, 12, 14).

While these mathematical models incorporated the best information then available, they rested upon pivotal assumptions that were shown subsequently to be erroneous (15–18). In particular, muscle was represented by its isometric force–length relationship. But being a characterization of muscle contraction in purely static circumstances, such a description is intrinsically incapable of broaching issues involving smooth muscle dynamics as occur during tidal breathing and deep inspirations (DIs). For example, as early as 1859 Salter (19) reported the following:

> . . .[bronchial] spasm may be broken through, and the respiration for the time rendered perfectly free and easy, by taking a long, deep, full inspiration. In severe asthmatic breathing this cannot be done; but in the slight bronchial spasm that characterizes hay asthma I have frequently witnessed it. It seems as if the deep inspiration overcame and broke through the contracted state of the air-tubes, which was not immediately re-established.

Subsequently we came to learn that of all innate agencies of bronchodilation the most potent of all is a DI (20), but in the asthmatic the ability of a DI to relax airway smooth muscle and dilate the airway is greatly attenuated (21–26). Indeed, Fish and coworkers (27) went so far as to suggest that the inability of an individual with asthma to dilate the airway with a DI might be the proximal cause of excessive airway narrowing in asthma.

Why is the individual with asthma, but not the normal subject, refractory to the potent bronchodilatory effects of a DI? And, more generally, what is the role of DIs in AHR? These questions involve airway dynamics, and here we have examined these questions experimentally; our strategy departed in two ways from those previously used. First, rather than using a theoretical description of muscle behavior as described above (11, 12, 14), here we studied smooth muscle shortening in the muscle bath. Second, as in previous approaches we used a mathematical description of the load against which the muscle is contracting; the load was dynamic rather than static, and this dynamic load was applied to real activated muscle through the agency of a servo-controller. As closely as possible, therefore, the ASM was loaded as it would be *in vivo.* The advantage of this hybrid strategy is that, first, it retains control of the many pathophysiologic factors that set the muscle load and, second, it makes no assumptions about the muscle itself. In contrast with previous investigations (11, 12, 14), muscle shortening can be observed directly rather than predicted theoretically. Here, however, we have adapted the approach of Latourelle and colleagues (28) so as to incorporate progressive remodeling of the different airway wall compartments.

As in many previous studies of AHR, results presented here again point to muscle mass as being the main culprit. However, these results show that mechanisms accounting for AHR are mainly dynamic and are therefore unaccounted for in previous theoretical analyses, which are static. Moreover, these results show that increased ASM mass not only explains AHR but also accounts for the failure of a DI to relax the asthmatic airway,

(*Received in original form November 7, 2006 and in final form April 4, 2007*)

This work was supported by National Heart, Lung, and Blood Institute grants HL-59682 and HL-33009 to J.J.F.

Correspondence and requests for reprints should be addressed to Jeffrey J. Fredberg, Ph.D., Harvard School of Public Health, 665 Huntington Avenue, Building 1, Room 1308, Boston, MA 02115. E-mail: jeffrey_fredberg@harvard.edu

Am J Respir Cell Mol Biol Vol 37. pp 264–272, 2007
Originally Published in Press as DOI: 10.1165/rcmb.2006-0418OC on April 26, 2007
Internet address: www.atsjournals.org

much as had been described by Salter (19). Indeed, these experiments imply that the failure of a DI to relax the asthmatic airway is the proximal cause of AHR.

MATERIALS AND METHODS

Setting the Muscle Load

We followed the approach of Latourelle and coworkers (28). In brief, airway smooth muscle was subjected to a virtual load created by a servo-controlled lever system (Cambridge Technologies, Lexington, MA, currently sold by Aurora Scientific, Aurora, Canada). The servo-controller was programmed using a mathematical model that closely approximates the *in vivo* dynamic loading conditions that are believed to prevail during normal spontaneous breathing. The mathematical model took into account the following factors: (*1*) airway wall geometry, (*2*) passive airway wall forces, (*3*) parenchymal interdependence, and (*4*) transpulmonary pressure, and its changes in time. For any given muscle strip in the bath, actual muscle mass was of course fixed, but we could simulate the effects of virtual increases in muscle mass by proportionate decreases in the servo-controlled real muscle load. The passive structures in the wall were modeled using pressure–area relationships described by Lambert and colleagues (29), which were based on experimental data from Hyatt and coworkers (30). We used their parameters for airway generation 8. Constants used for calculating forces due to the passive structures of the airway wall were as follows: $\alpha_o = 0.213$, $\alpha_o' = 0.174$, $n_1 = 1$, $n_2 = 10$, $A_m = 10.2$ cm^2 (29). The contribution of parenchymal distortion to muscle load was calculated using the shear modulus of lung parenchyma, μ, and the change in adventitial diameter (31); distortion of lung parenchyma imposes an increased load on the airway smooth muscle as it shortens. The shear modulus depends directly upon transpulmonary pressure, P_L, according to the relationship $\mu = 0.7\ P_L$(32). Transpulmonary pressure, smooth muscle force, and airway radius were directly related using the Laplace relationship in a thin-walled cylinder. Changes in adventitial diameter were related to changes in muscle length as described by Lambert and colleagues (12). These formulations of the load characteristics have already been described in detail (28). To vary airway wall geometry we used the relationships between airway size and different airway wall components described by Lambert and coworkers (12). The airway wall was subdivided into submucosal, smooth muscle, and adventitial wall areas and incorporated into the model. We could then control the thickness of each of these individual compartments to simulate remodeling of the asthmatic airway. We used the slope and intercept values for the regression of wall areas on basement membrane perimeter provided by Lambert and colleagues (12) for these calculations.

Experimental Protocol

The sheep tracheal smooth muscle strip was mounted in a muscle bath (Krebs-Henseleit solution, 37°C, aerated with 95% O_2–5% CO_2, pH 7.3–7.5) and set to a reference length (L_{ref}) for optimal response in the standard manner using electric field stimulation (EFS). The reference length L_{ref} was set as the length at which the response to an EFS, 5 min after a 0.5-mm length increase, differed by $< 10\%$ when compared with the response at the previous length. After 45 min at L_{ref}, the muscle was activated with acetylcholine chloride (ACh) and allowed to contract isometrically for 30 min. The concentration of ACh was maintained at 10^{-4} M by constantly pumping fresh solution in to muscle bath. The force generated by the muscle at the end of the 30 min of isometric contraction was denoted as F_{ref}. ACh was then washed out and the muscle returned to a relaxed state.

In designing our experimental protocol, tidal breathing might have been imposed either before or after initiating the contractile stimulus. The former choice is certainly physiologic but would not allow us to obtain the appropriate control state for this particular study, which was designed to compare muscle lengths equilibrated in statically loaded versus dynamically loaded circumstances. We opted, therefore, for the latter choice, with which we were able to create a well-defined statically equilibrated control state upon which tidal loading could then be superposed. In addition, we could use each strip as its own control.

We fixed P_L at 4 cm H_2O to simulate the load during static conditions, activated the muscle with ACh (maintained at 10^{-4} M), and allowed the muscle to shorten for 120 min to its static equilibrium length (L_{SE}). We then simulated the effect of quiet breathing with occasional deep inspirations by imposing sinusoidal fluctuations of P_L (amplitude of 1.25 cm H_2O) at 12 breaths/min, with a single deep breath (a positive half sine of amplitude $\Delta P_L = 10$ cm H_2O) every 6 min.

Normalization

We used three steps to normalize the experimental data. (*1*) We first normalized the load characteristics in the following manner. For any given P_L, smooth muscle length was plotted as a fraction of L_o, which was defined as the radius of the relaxed smooth muscle (i.e., when active force is zero) at a P_L of 10 cm H_2O. The force was normalized to F_o, which was defined as the maximum force the muscle can generate. F_o was computed using the thickness of the smooth muscle at L_o and an estimated maximal stress the smooth muscle is capable of generating (we used 150 kPa [12]). (*2*) We then scaled the experimental L_{ref} and F_{ref} to L_o and F_o. (*3*) Finally, we normalized the experimental force and length to the re-scaled L_{ref} and F_{ref}.

Muscle Activation, Mass, and Force Generation Capacity

We used only one level of agonist concentration: ACh at 10^{-4} M. Graded levels of muscle activation, mass, and different force generation capacities of the muscle were simulated by the servo-controller, which used an activation factor. The activation factor scaled the load in proportion to the F_{ref} of the actual muscle that is in the bath. However, muscle edema or swelling, rather than variations in muscle accumulation, could not be addressed in our protocol.

Geometry of Wall Compartments

To study the contributions of the different compartments of airway wall we measured changes in muscle length after replacing one of each of the compartments with modified values. In this manner we studied the effect of thickening the smooth muscle layer, the adventitial layer, or the submucosal layer. Similar to Lambert *et al.* (12) we did not move the luminal boundary inward while increasing the submucosal thickness.

Deep Inspirations

DI amplitude was increased from 0 to 30 cm H_2O in steps of 5 cm H_2O every 30 min.

Statistical Analysis

Different protocols used different numbers of strips (n). All data were expressed as mean ± SE. To evaluate the differences between means, *t* tests and ANOVA were performed using EXCEL.

RESULTS

Load Characteristics

The load characteristic is the elastic loading force, F, against which the smooth muscle would have to contract to attain a given muscle length, L. Being a property of the load and not the muscle, the load characteristic is determined by airway geometry, airway wall properties, tethering of the airway to the lung parenchyma, and the P_L. As has been shown by others previously (12, 14, 33), load characteristics for normal airway (Figure 1, *dark lines*) and asthmatic airway (Figure 1, *light lines*) show dramatic differences.

We begin by considering only one of these load characteristics, the case of the normal airway with P_L held fixed at 4 cm H_2O. If muscle force is zero then the muscle length will be close to 0.9 L_o. As muscle force increases, muscle length decreases, following a sigmoidal relationship until, at $\sim 0.3\ L_o$, muscle shortening becomes limited by airway closure. Increasing P_L causes the relationship to shift upward and to the right, indicating that greater muscle force would be required to attain any given muscle length, but because airway closure is set by mainly geometrical factors, it is insensitive to P_L. Moreover, airway closure occurs while F remains less than F_o, indicating that even in

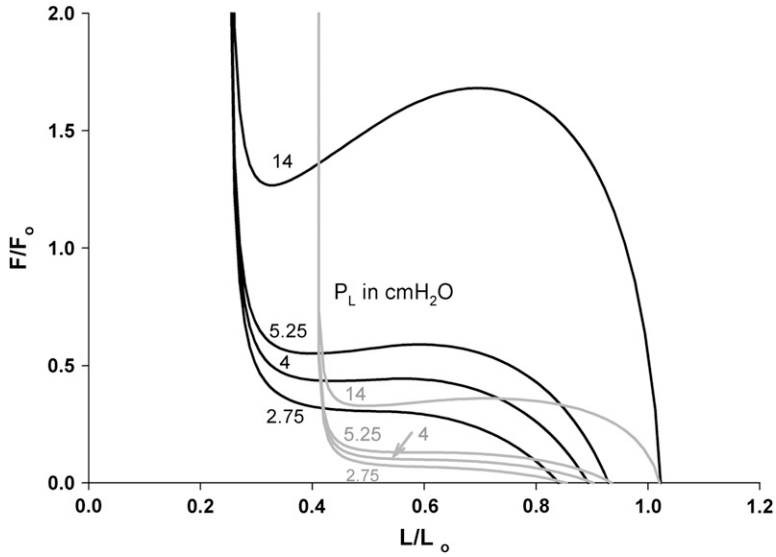

Figure 1. Load characteristics for different transpulmonary pressures (P_L) from normal muscle (*dark lines*) and asthmatic muscle (*light lines*). Smooth muscle length L was plotted as a fraction of L_o (radius of relaxed smooth muscle at a P_L of 10 cm H_2O) and active force F was plotted as a fraction of F_o (maximum force the muscle can generate, computed using the thickness of the smooth muscle at L_o and an estimated maximal stress of 150 kPa [12]). If the muscle generates a very high force, the airways are almost completely closed. If the muscle generates no force, the airways are nearly open. In between these extremes, the muscle force and length depend on pleural pressure, that is, the force and length of the muscle must lie on this line. Unlike the normal airway, the asthmatic airway already closes at a muscle length of 0.4 L_o, and muscle shortening requires much less force.

the normal airway, activated muscle has the force-generating capacity to close the airway (34).

In the asthmatic airway each of the airway compartments are thickened, and as a result corresponding geometric factors are altered and the load characteristics are shifted down and to the right. For the same P_L = 4 cm H_2O, if muscle force is zero then muscle length is about the same as in the normal airway, but as muscle force increases muscle length decreases far more than in the normal lung. Moreover, muscle shortening becomes limited at a substantially greater muscle length, and that limitation occurs at a dramatically smaller muscle force.

Static Loading

Using the servo-controller, we loaded airway smooth muscle with the characteristic shown in Figure 1 for the case of P_L held fixed at 4 cm H_2O. We then activated the muscle maximally using 10^{-4} M ACh. Such a contraction is neither isometric nor isotonic, but rather is auxotonic and much closer to the realistic physiology. The trajectory of muscle shortening (Figure 2A, and on an expanded scale in Figure 2C) begins at point A and follows the load characteristic until shortening eventually stops at point B, at which point the elastic load is balanced by the steady-state active force generated by the muscle. We allowed 120 min for muscle shortening to be completed and the system to come to this balance of static forces. Compared with the normal airway, in the asthmatic airway the smooth muscle shortened far more (Figures 2B and 2D).

Dynamic Loading

After 120 min of auxotonic shortening against a fixed load characteristic (point B, Figure 2C), we initiated changes of transpulmonary pressure in time mimicking the pattern of normal respiration, namely, tidal breathing punctuated by occasional DIs (35).

These changes of P_L caused the load characteristic to change smoothly in time between isopleths shown in Figure 1. The response to a DI was as follows. As P_L reached a maximum of 14 cm H_2O, the trajectory (B to C) shows that force grew substantially and exceeded F_{ref} for much of the time and muscle length increased appreciably. As P_L returned to 4 cm H_2O, the muscle shortened from C back to point D′, and over the next few tidal breathing it shortened further (from D′ to D). However, as tidal breathing continued the muscle re-lengthened (in a looping trajectory) and the mean muscle force slowly decreased (D to E, *blue*). After 6 min, this slow lengthening was interrupted by the second DI, whereupon the muscle followed the trajectory EFG (*pink*). As tidal breathing and DIs continued, the muscle became equilibrated on a dynamic trajectory approximating G. At all points on this dynamic trajectory, muscle length far exceeded the muscle length at the statically equilibrated value indicated by point B.

To better visualize muscle shortening in response to this loading pattern, we calculated the average muscle length over the duration of a single breath and plotted it against time. Results from a representative muscle are shown in Figure 3 (points B to G are marked for reference to Figure 2). After 2 h of static loading, the muscle in the asthmatic airway had shortened much more than the muscle in the normal airway ($P < 0.05$). In the normal airway, the first DI caused muscle to lengthen substantially and had a long-lasting effect; muscle length became dynamically equilibrated. In contrast, muscle in asthmatic airway was shorter and refractory to the effects of DIs. Each DI caused only a small increase in muscle length, the effect was short-lived, and after the DI was completed the muscle quickly returned to its static frozen state.

In the normal airway (Figures 2C and 3, *dark line*), DIs and tidal breathing are thus seen to exert potent bronchodilatory effects. The first DI caused the muscle to lengthen by ~ 20%, and continued tidal breathing and DIs resulted in more lengthening. After 30 min of breathing and DI, the muscle lengthened from its static value of 0.66 ± 0.04 to 0.84 ± 0.01 ($P < 0.01$). By contrast, in the asthmatic airway (Figures 2D and 3, *light line*) the effects of DIs and tidal breathing were dramatically attenuated. The first DI caused the muscle to lengthen only by 5%, and by the time of the next deep inspiration 6 min later, the muscle had shortened almost back to where it was under static conditions. The muscle in this case made comparatively smaller force length excursions and appeared to be stuck at a small length (static 0.52 ± 0.05 and 0.53 ± 0.05 after 30 min of breathing with DI).

During dynamic loading, differences in muscle length between the asthmatic and normal airway became progressively smaller as muscle activation was decreased (Figure 4). However, in the normal airway changes of muscle length with change of activation were slight, whereas in the asthmatic airway they were substantial. *Error bars* denote SE between muscle strips and

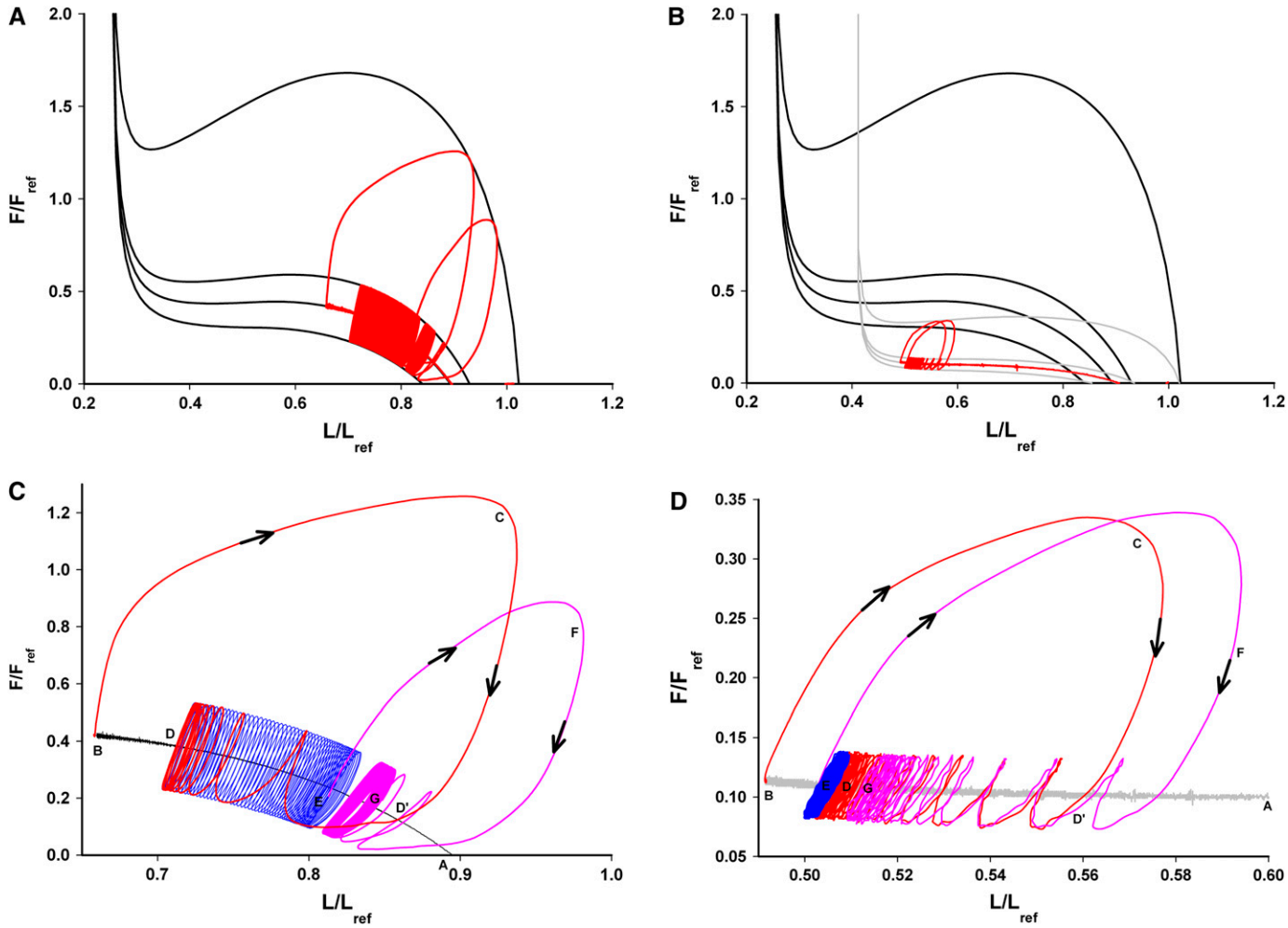

Figure 2. Force–length measurements from tracheal smooth muscle strips (*red lines*) and corresponding load characteristics (*light* and *dark lines*) for normal (*A*, *C*) and asthmatic airways (*B*, *D*). Activated muscle strips were statically equilibrated for 2 h at P_L of 4 cm H_2O, after which tidal breathing was imposed (sinusoidal fluctuations of amplitude 1.25 cm H_2O with a single breath of amplitude 10 cm H_2O every 6 min). A was the starting point, where the muscle was completely relaxed. After 2 h of static loading, the muscle shortened from A to B. BCD was the response to the first DI, and continued breathing opened the airways from D to E. EFG was the response to the second DI, and the airway continued to relax. Overall, the muscle was driven toward progressively greater lengths and smaller forces. In contrast, asthmatic airways did not lengthen between DIs (E < D). The airways appeared to be stuck at static levels, and the smooth muscle experienced smaller force–length excursions.

asterisk indicates a significant difference between the normal and asthmatic conditions ($P < 0.05$) at each level of activation. The *dagger symbol* indicates that for the normal muscle, there was a significant difference between its static equilibrium length and the length after 30 min of breathing and DI ($P < 0.01$). Importantly, the asthmatic loading condition (relative to normal) reflects not only AHR (excessive narrowing) but also hypersensitivity (substantial narrowing at low levels of muscle activation).

Muscle Contractility

Against a steady load characteristic, muscle shortening increased progressively as muscle contractility increased (Figure 5). However, against a dynamic load, muscle shortening changed little up to a 2-fold increase in contractility. For greater increases of contractility and 100% muscle activation, muscle shortened to static levels.

Airway Wall Geometry

During static loading, the statically equilibrated muscle length was sensitive to the thickness of the wall layers (Figure 6). However, when compared with thickening of only submucosal (to $0.67L_{ref}$) or only adventitial (to $0.62L_{ref}$) compartments, thickening of the smooth muscle layer alone produced the greatest muscle shortening (to $0.47L_{ref}$) ($P < 0.01$). During dynamic loading, the airway with thickened submucosal and adventitial layers ASM lengthened dramatically (to 0.83 L_{ref}) ($P < 0.01$), but DIs and tidal breathing failed to lengthen ASM with increased ASM mass. Only when the thickness of the smooth muscle layer decreased down to normal values did the muscle re-lengthen. Of these three airway compartments, therefore, by far the most important contributor was the thickness of the muscle compartment.

DI Magnitude

When DIs were included, the normal airway equilibrated at muscle lengths that were greater as the amplitude of the DIs increased, but amplitudes in excess of 20 cm H_2O did not cause any more relaxation (Figure 7). In the asthmatic airway, by contrast, the muscle remained virtually stuck at its statically equilibrated lengths even after DIs were introduced ($P < 0.01$),

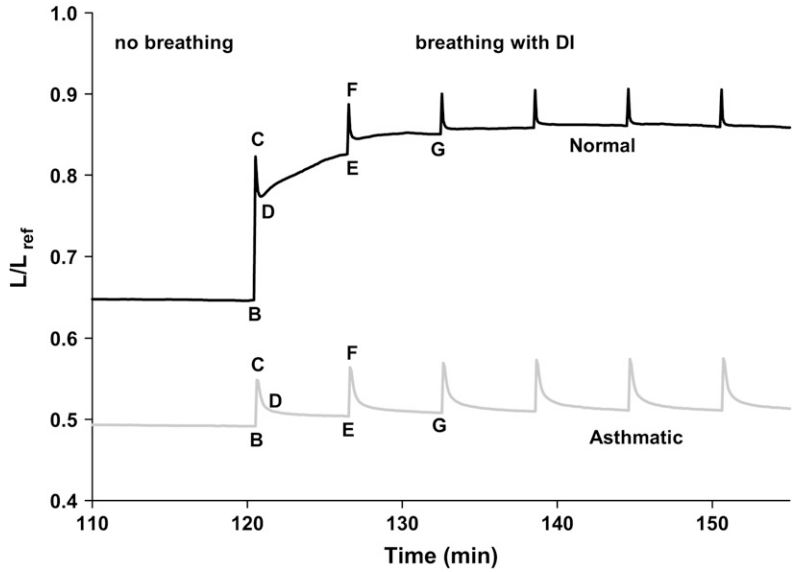

Figure 3. Muscle length (averaged over the duration of one breath) versus time. When breathing and deep inspiration started, the normal airway (*dark line*) dilated in response to a DI and remained dilated, whereas the asthmatic airway (*light line*) only dilated by a small amount and quickly returned to its static state.

and lengthened only in response to DI amplitudes of 20 cm H_2O or more.

DISCUSSION

In this report we focused upon the muscle load, the muscle mass, and the implications of changes in these features in airway narrowing in asthma. During imposed tidal breathing and DIs, but not during static loading conditions, altered airway wall geometry caused ASM to recapitulate cardinal features of asthma, including AHR, airway hypersensitivity, and the failure of a deep inspiration to reverse airway narrowing. Within the first three DIs, maximally activated ASM in the normal airway lengthened appreciably, whereas that in the asthmatic airway remained stuck at a small muscle length. When compared with the effects of thickening of submucosal or adventitial compartments, it was

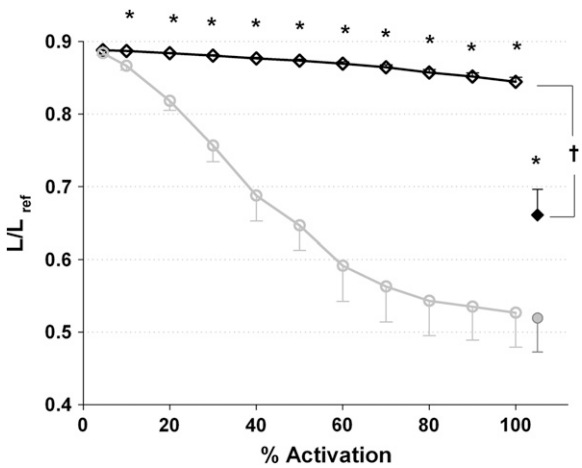

Figure 4. Muscle length averaged over one breath versus %activation in normal and asthmatic airways ($n = 5$ for each type of airway). After 30 min of full activation, the activation level was gradually reduced. This was simulated by equating the full force produced by the muscle to less and less tensile stress. While the normal airway is almost fully dilated after the first two DIs (significant when compared with the corresponding static values, $^{\dagger}P < 0.01$), the asthmatic airway showed very little reaction. Only when the activation level was decreased below 15% did the asthmatic muscle lengthen to a level that was observed in normal airways at 100% activation. *Error bars* denote SE between muscle strips and the *asterisk* indicates a significant difference between the normal and asthmatic conditions ($P < 0.05$) at each level of activation.

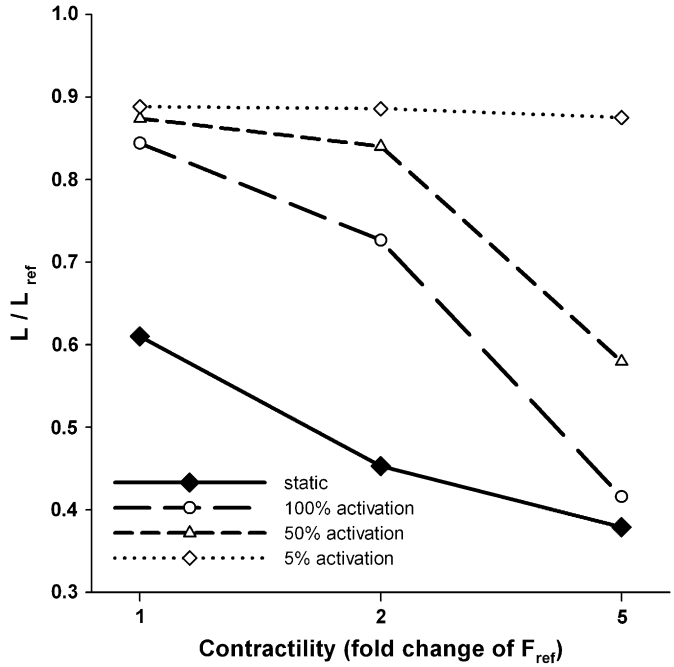

Figure 5. Muscle length averaged over one breath versus contractility in normal airways ($n = 3$). Three different levels of force generation were used. The muscle was loaded statically for 2 h, after which breathing with DI was turned on. After 30 min of breathing, the activation level was gradually reduced. In response to static loading, the smooth muscle with the greatest force-generating capacity shortened the most. In response to breathing and DI, the muscle with increased force-generating capacity (5-fold) behaved like an asthmatic muscle and remained short till it was deactivated below 15%.

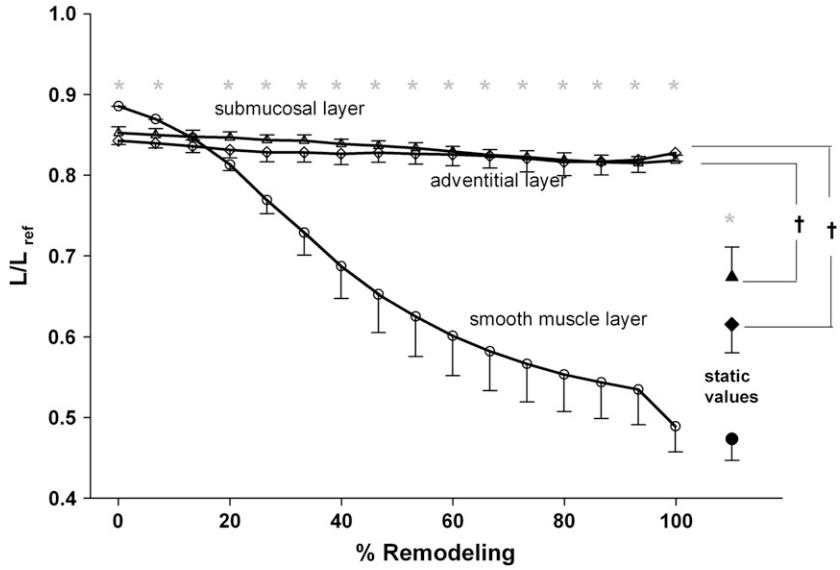

Figure 6. Muscle length averaged over one breath versus remodeling ($n = 4$ for each layer). After 2 h of static loading and 30 min of breathing, each layer was "unremodelled" individually. In response to static loading, the airway with asthmatic smooth muscle layer shortened the most ($P < 0.01$). The smooth muscle layer played the greatest role in reproducing hyperresponsiveness when compared with adventitial and submucosal layers. *Error bars* denote SE between muscle strips and the *asterisk* indicates a significant difference ($P < 0.01$) between the three different layers. The *dagger* indicates a significant difference ($P < 0.01$) between the static equilibrium values and the response to 30 min of breathing and DI for the adventitial and submucosal layers.

thickening of the smooth muscle layer that produced the greatest ASM shortening.

These findings reinforce the long-held conclusion that the functionally dominant derangement accounting for AHR is increased smooth muscle mass. In doing so, however, these findings establish that the main mechanisms underlying AHR are intrinsically dynamic, and are therefore unaccounted for in previous theoretical models, which are intrinsically static. Moreover, these findings replicate not only the potent bronchodilatory effects of DIs but also the failure of DIs to dilate the asthmatic airway, much as had been described by Salter (19) more than 150 years ago but had remained since that time unexplained. Indeed, these experiments imply that the failure of a DI to relax the asthmatic airway is the proximal cause of AHR.

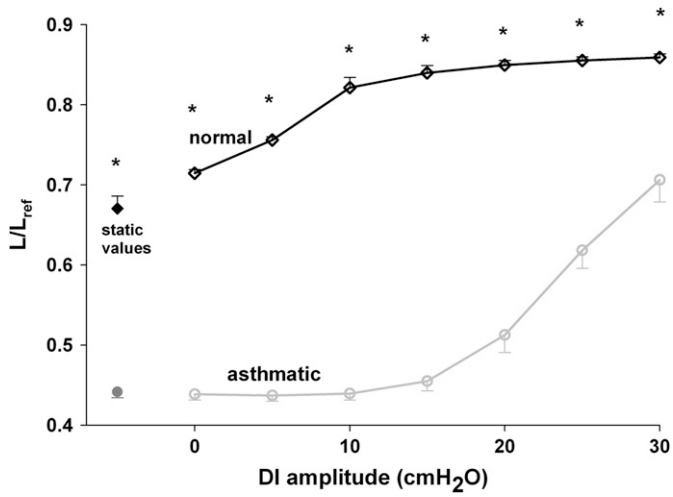

Figure 7. Muscle length averaged over one breath versus DI amplitude in normal and asthmatic airways ($n = 4$ for each case). After 2 h of static loading at $P_L = 4$ cm H_2O, tidal breathing (sinusoidal fluctuations of amplitude 1.25 cm H_2O) was imposed. There was no DI for the first 30 min. Thereafter a DI was introduced every 6 min. The DI amplitude was varied in steps of 5 cm H_2O, from 5–30 cm H_2O, every 30 min. In response to breathing the muscle in the normal airway lengthened immediately (even in the absence of DI) and it continued lengthening by a small amounts with increasing DI amplitudes. The muscle in the asthmatic airway remained at static lengths and only lengthened in response to a DI amplitude of 20 cm H_2O and more. *Error bars* denote SE between muscle strips, and the *asterisk* indicates a significant difference between the normal and asthmatic conditions ($P < 0.01$) at each DI amplitude.

In the remainder of this section we highlight reasons that previous static analyses fail to provide an adequate description of AHR, and then go on to describe the essential dynamics that are now seen to control airway narrowing.

Why Do Previous Analyses Fail?

It had been widely assumed that during bronchospasm the airway continues to narrow until the active force generated by ASM comes into balance with the passive elastic load against which the muscle is contracting (11, 12, 14); the ASM had been assumed to be statically equilibrated. But since those models were published we have subsequently learned that this assumption is not even approximately correct (16, 36–38). To represent force generated by ASM, mathematical models that have been used previously begin with the classical static force–length curve. However, spontaneous breathing causes tidal lung expansion, and tidal lung expansion causes tidal stretches of airway smooth muscle. Even though they are only a few percent of muscle length, these small stretches are transmitted to the myosin head and are large enough to cause it to detach from actin much sooner than it would have during an isometric contraction (15, 16, 39–41). Thus, these small tidal stretches perturb the binding of myosin to actin, dramatically reduce the myosin duty cycle, and thereby cause active forces generated by the muscle to be far smaller than they would be during an isometric contraction with the same degree of activation and the same mean muscle length. As a result, instantaneous muscle force is not constrained to lie upon the classical static force–length curve or the classical Hill force–velocity curve. Even when the mean muscle load is the same, differences in muscle response to static versus time varying loading conditions are rather dramatic, as illustrated in Figure 3.

Moreover, we have also come to learn that ASM can adapt its static force–length curve rather dramatically, and can do so on time scales as short as hours, minutes, or even seconds (37, 38, 42). The mechanisms of cytoskeletal remodeling that account

for that adaptation are not well understood and are the subject of much current attention (42, 43). It is clear, however, that the classical force–length curve and its associated optimal length, if they exist at all, are not particularly relevant to the question of airway narrowing in asthma. Rather, through the actions of cytoskeletal remodeling the airway smooth muscle cell has the capacity to generate the same high static force over a huge range of muscle lengths, and for that reason the classical force–length curve, the optimal length, and the models that rest upon them engender errors that are not small.

Dynamics of Airway Narrowing: a New Synthesis

Before 1992 the picture of airway narrowing was qualitative and predicted intuitively that greater muscle mass would lead to greater active force and, hence, greater airway narrowing (Figure 8A). Wiggs and coworkers (11) and Lambert and colleagues (12) performed the first quantitative analyses of airway narrowing (Figure 8B). Although remodeling of various airway compartments were shown to decrease the load and thus contribute importantly to the extent of airway narrowing, the dominant effect was found to be increased muscle mass.

In the mid-1990 s many investigators recognized that tidal loading is a potent inhibitor of active muscle force (15, 20, 36, 44, 45) (Figure 8C). While this picture helped to explain why tidal breathing and deep inspirations are potent bronchodilators, it failed to explain why individuals with asthma are refractory to the beneficial effects of a DI. Finally, it was recognized that if muscle mass becomes too large or imposed force fluctuations become too small, then ASM stiffens and therefore stretches less, and because it stretches less it stiffens even more (15, 16, 39, 40, 46), and so on. This vicious positive feedback (Figure 8D) causes the system to collapse to a statically equilibrated state; the ASM

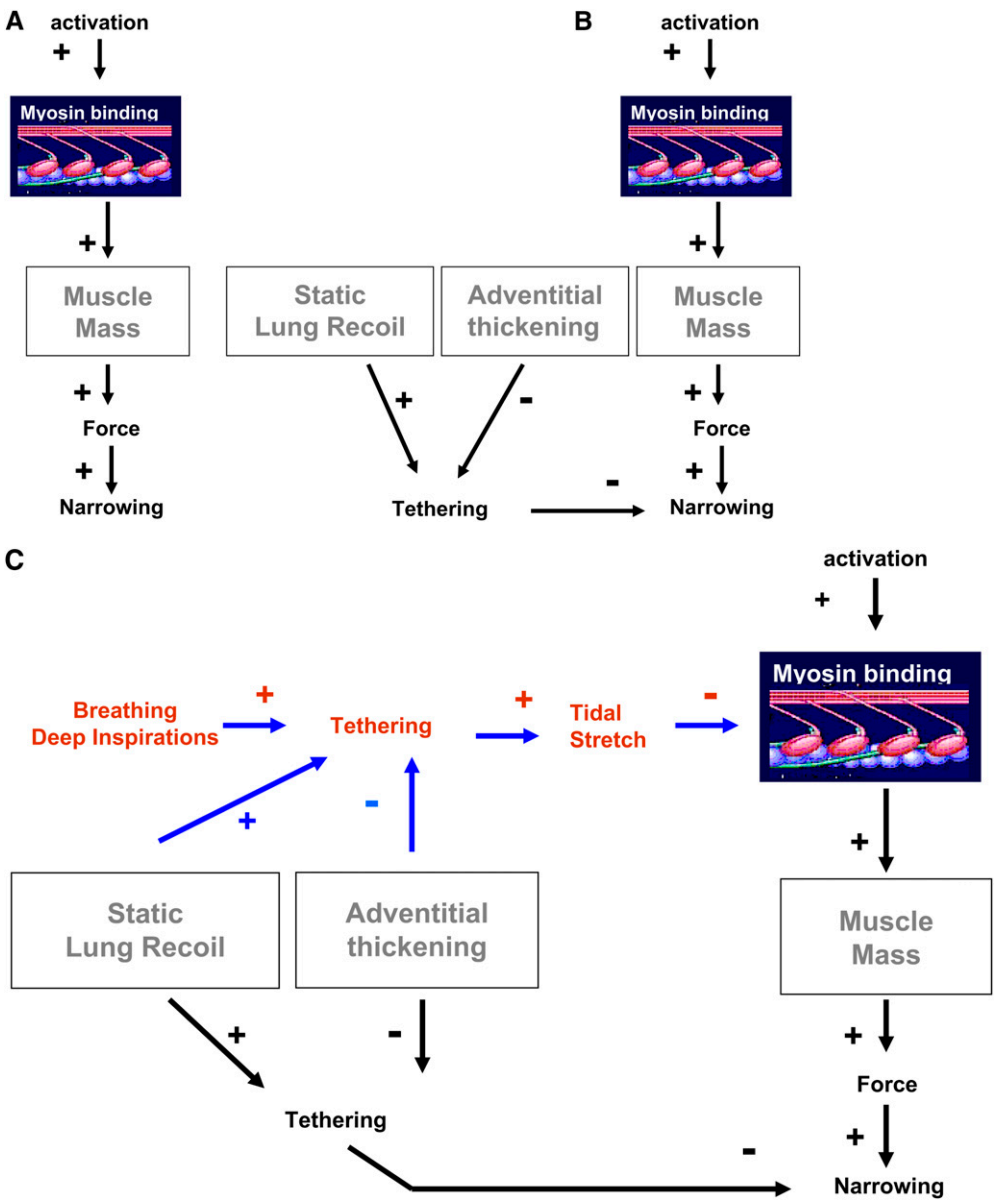

Figure 8. (*A*) The qualitative picture before 1992: the picture of airway narrowing was qualitative but predicted intuitively that greater muscle mass would lead to greater active force and, hence, greater airway narrowing. (*B*) Balance of static forces: Wiggs and colleagues (11) and Lambert and coworkers (12) performed the first quantitative analysis of airway narrowing. Their analysis rests upon a balance of static forces, with muscle length being set by the balance of active force generated by the muscle versus the passive elastic load against which the muscle is shortening. Although remodeling of various airway compartments were shown to decrease the load and thus contribute importantly to the extent of airway narrowing, the dominant effect was increased muscle mass. (*C*) Tidal loading: In the mid-1990s many investigators recognized that tidal loading is a potent inhibitor of active muscle forces. While this picture helped to explain why tidal breathing and deep inspirations are potent bronchodilators, it failed to explain why individuals with asthma are refractory to the beneficial effects of a DI. (*D*) Myosin dynamics: Due to a virtuous positive feedback loop, breathing is seen to be good for breathing. This positive feedback ensures that, even during maximal muscle stimulation, tidal stretches and/or DIs act to perturb the binding of myosin to actin, and thus keep active force and muscle stiffness quite small. Small muscle stiffness, in turn, keeps the muscle highly responsive to tidal loading, and so on. However, with decreased static lung recoil, increased adventitial thickening, or, especially, increased muscle mass, the myosin binding is perturbed less, the muscle becomes stiffer as a result, and stretches even less, and so on. The feedback loop collapses and the muscle becomes so stiff as to be refractory to the effects of DIs. "+" and "−," respectively, indicate phenomena that act to increase or decrease the indicated effect. For example, adventitial thickening decreases tethering forces, and tethering forces act to decrease the extent airway narrowing. By decreasing tethering, therefore, adventitial thickening acts to exacerbate airway narrowing.

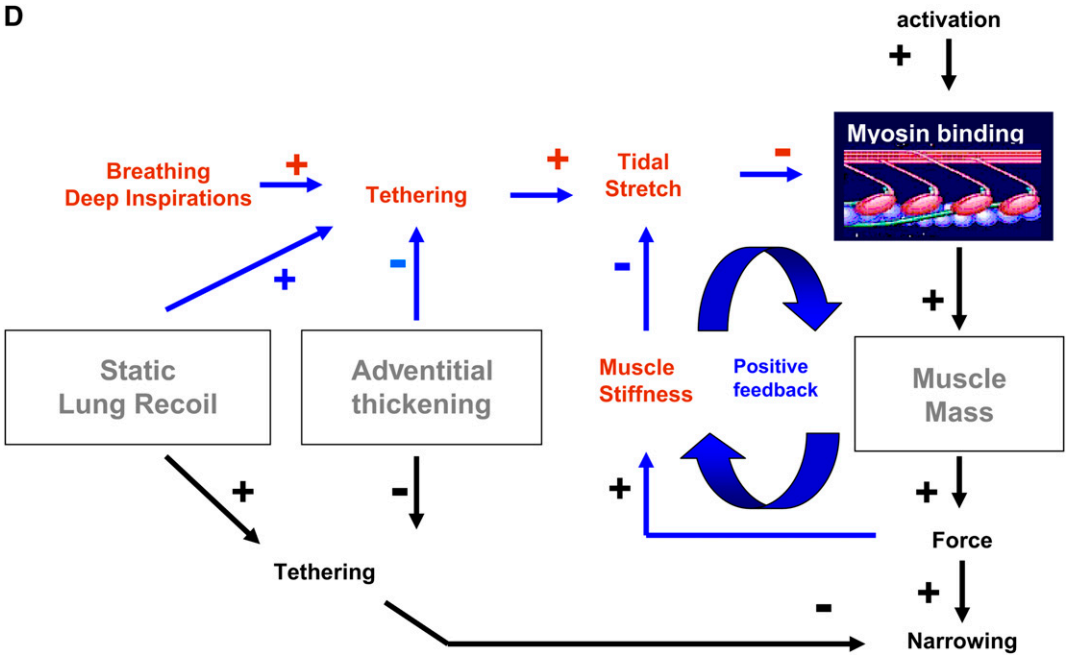

Figure 8. Continued.

virtually freezes in the latch state, and becomes so stiff that tidal breathing and DIs can no longer perturb myosin binding.

Indeed, we have recently come to learn that the contracted airway smooth muscle cell becomes refractory to a DI because its cytoskeleton fails to fluidize, and instead remains frozen in a stiff solid-like phase (47, 48).

In conclusion, we have shown here that increased ASM mass has the potential to dominate the mechanical response of the remodeled asthmatic airway, and that ASM dynamics play a crucial role in that process. Nonetheless, several questions remain open. Neural or humoral mechanisms associated with DIs cannot be ruled out, and we did not address here differences in the muscle cell itself. For example, An and coworkers have recently studied ASM cells obtained from the relatively hyperresponsive Fisher rat and the relatively hyporesponsive Lewis rat (49). They found that differences in muscle contractility and other physical differences measured at the level of the single cell *in vitro* were consistent with strain-related differences in airway responsiveness *in vivo*. These observations highlight the fact that it remains unclear if muscle mass and muscle contractility might co-vary. It is possible, moreover, that the ASM cell in the proliferative/synthetic/maturational state might be less contractile than similar cells differentiated into fully the contractile state—an effect that would be compensatory—but no mechanical data are yet available to support that possibility. The effects of time varying mechanical loads upon ASM proliferation, phenotype, or matrix deposition, composition, and mechanical properties remain unclear as well.

Conflict of Interest Statement: None of the authors has a financial relationship with a commercial entity that has an interest in the subject of this manuscript.

References

1. Woolcock AJ, Peat JK. Epidemiology of bronchial hyperresponsiveness. *Clin Rev Allergy* 1989;7:245–256.
2. McParland BE, Macklem PT, Pare PD. Airway wall remodeling: friend or foe? *J Appl Physiol* 2003;95:426–434.
3. Macklem PT. Mechanical factors determining maximum bronchoconstriction. *Eur Respir J Suppl* 1989;6:516s–519s.
4. Sterk PJ, Bel EH. Bronchial hyperresponsiveness: the need for a distinction between hypersensitivity and excessive airway narrowing. *Eur Respir J* 1989;2:267–274.
5. Bai TR, Knight DA. Structural changes in the airways in asthma: observations and consequences. *Clin Sci (Lond)* 2005;108:463–477.
6. Brusasco V, Pellegrino R. Complexity of factors modulating airway narrowing in vivo: relevance to assessment of airway hyperresponsiveness. *J Appl Physiol* 2003;95:1305–1313.
7. Fredberg JJ. Bronchospasm and its biophysical basis in airway smooth muscle. *Respir Res* 2004;5:2.
8. Pare PD, Roberts CR, Bai TR, Wiggs BJ. The functional consequences of airway remodeling in asthma. *Monaldi Arch Chest Dis* 1997;52:589–596.
9. King GG, Pare PD, Seow CY. The mechanics of exaggerated airway narrowing in asthma: the role of smooth muscle. *Respir Physiol* 1999;118:1–13.
10. Martin JG, Duguet A, Eidelman DH. The contribution of airway smooth muscle to airway narrowing and airway hyperresponsiveness in disease. *Eur Respir J* 2000;16:349–354.
11. Wiggs BR, Bosken C, Pare PD, James A, Hogg JC. A model of airway narrowing in asthma and in chronic obstructive pulmonary disease. *Am Rev Respir Dis* 1992;145:1251–1258.
12. Lambert RK, Wiggs BR, Kuwano K, Hogg JC, Pare PD. Functional significance of increased airway smooth muscle in asthma and COPD. *J Appl Physiol* 1993;74:2771–2781.
13. Macklem PT. The mechanics of breathing. *Am J Respir Crit Care Med* 1998;157:S88–S94.
14. Macklem PT. A theoretical analysis of the effect of airway smooth muscle load on airway narrowing. *Am J Respir Crit Care Med* 1996;153:83–89.
15. Fredberg JJ, Inouye D, Miller B, Nathan M, Jafari S, Raboudi SH, Butler JP, Shore SA. Airway smooth muscle, tidal stretches, and dynamically determined contractile states. *Am J Respir Crit Care Med* 1997;156:1752–1759.
16. Fredberg JJ, Inouye DS, Mijailovich SM, Butler JP. Perturbed equilibrium of myosin binding in airway smooth muscle and its implications in bronchospasm. *Am J Respir Crit Care Med* 1999;159:959–967.
17. Dowell ML, Lakser OJ, Gerthoffer WT, Fredberg JJ, Stelmack GL, Halayko AJ, Solway J, Mitchell RW. Latrunculin b increases force fluctuation-induced relengthening of ach-contracted, isotonically shortened canine tracheal smooth muscle. *J Appl Physiol* 2005;98:489–497.
18. Lakser OJ, Lindeman RP, Fredberg JJ. Inhibition of the p38 map kinase pathway destabilizes smooth muscle length during physiological loading. *Am J Physiol Lung Cell Mol Physiol* 2002;282:L1117–L1121.

19. Salter HH. Classic papers in asthma: on asthma, its pathology and treatment, 1859. In: Brewis RAL, editor. The evolution of understanding, vol. 1. London: Science Press Limited; 1990. pp. 106–142.
20. Gump A, Haughney L, Fredberg J. Relaxation of activated airway smooth muscle: relative potency of isoproterenol vs. Tidal stretch. *J Appl Physiol* 2001;90:2306–2310.
21. Fish JE, Peterman VI, Cugell DW. Effect of deep inspiration on airway conductance in subjects with allergic rhinitis and allergic asthma. *J Allergy Clin Immunol* 1977;60:41–46.
22. Skloot G, Permutt S, Togias A. Airway hyperresponsiveness in asthma: a problem of limited smooth muscle relaxation with inspiration. *J Clin Invest* 1995;96:2393–2403.
23. King GG, Moore BJ, Seow CY, Pare PD. Time course of increased airway narrowing caused by inhibition of deep inspiration during methacholine challenge. *Am J Respir Crit Care Med* 1999;160:454–457.
24. Lim TK, Ang SM, Rossing TH, Ingenito EP, Ingram RH Jr. The effects of deep inhalation on maximal expiratory flow during intensive treatment of spontaneous asthmatic episodes. *Am Rev Respir Dis* 1989; 140:340–343.
25. Scichilone N, Pyrgos G, Kapsali T, Anderlind C, Brown R, Permutt S, Togias A. Airways hyperresponsiveness and the effects of lung inflation. *Int Arch Allergy Immunol* 2001;124:262–266.
26. Wheatley JR, Pare PD, Engel LA. Reversibility of induced bronchoconstriction by deep inspiration in asthmatic and normal subjects. *Eur Respir J* 1989;2:331–339.
27. Fish JE, Ankin MG, Kelly JF, Peterman VI. Regulation of bronchomotor tone by lung inflation in asthmatic and nonasthmatic subjects. *J Appl Physiol* 1981;50:1079–1086.
28. Latourelle J, Fabry B, Fredberg JJ. Dynamic equilibration of airway smooth muscle contraction during physiological loading. *J Appl Physiol* 2002;92:771–779.
29. Lambert RK, Wilson TA, Hyatt RE, Rodarte JR. A computational model for expiratory flow. *J Appl Physiol* 1982;52:44–56.
30. Hyatt RE, Wilson TA, Bar-Yishay E. Prediction of maximal expiratory flow in excised human lungs. *J Appl Physiol* 1980;48:991–998.
31. Lambert RK, Wilson TA. A model for the elastic properties of the lung and their effect of expiratory flow. *J Appl Physiol* 1973;34:34–48.
32. Lai-Fook SJ, Hyatt RE, Rodarte JR. Effect of parenchymal shear modulus and lung volume on bronchial pressure-diameter behavior. *J Appl Physiol* 1978;44:859–868.
33. Moreno RH, Hogg JC, Pare PD. Mechanics of airway narrowing. *Am Rev Respir Dis* 1986;133:1171–1180.
34. Brown RH, Herold CJ, Hirshman CA, Zerhouni EA, Mitzner W. Individual airway constrictor response heterogeneity to histamine assessed by high-resolution computed tomography. *J Appl Physiol* 1993;74: 2615–2620.
35. Bendixen HH, Smith GM, Mead J. Pattern of ventilation in young adults. *J Appl Physiol* 1964;19:195–198.
36. Shen X, Wu MF, Tepper RS, Gunst SJ. Mechanisms for the mechanical response of airway smooth muscle to length oscillation. *J Appl Physiol* 1997;83:731–738.
37. Pratusevich VR, Seow CY, Ford LE. Plasticity in canine airway smooth muscle. *J Gen Physiol* 1995;105:73–94.
38. Gunst SJ, Meiss RA, Wu MF, Rowe M. Mechanisms for the mechanical plasticity of tracheal smooth muscle. *Am J Physiol* 1995;268:C1267–C1276.
39. Fredberg JJ. Frozen objects: small airways, big breaths, and asthma. *J Allergy Clin Immunol* 2000;106:615–624.
40. Fredberg JJ. Airway smooth muscle in asthma: perturbed equilibria of myosin binding. *Am J Respir Crit Care Med* 2000;161:S158–S160.
41. Fredberg JJ, Jones KA, Nathan M, Raboudi S, Prakash YS, Shore SA, Butler JP, Sieck GC. Friction in airway smooth muscle: Mechanism, latch, and implications in asthma. *J Appl Physiol* 1996;81:2703–2712.
42. Seow CY, Pratusevich VR, Ford LE. Series-to-parallel transition in the filament lattice of airway smooth muscle. *J Appl Physiol* 2000;89:869–876.
43. Bursac P, Lenormand G, Fabry B, Oliver M, Weitz DA, Viasnoff V, Butler JP, Fredberg JJ. Cytoskeletal remodelling and slow dynamics in the living cell. *Nat Mater* 2005;4:557–561.
44. Gunst SJ. Contractile force of canine airway smooth muscle during cyclical length changes. *J Appl Physiol* 1983;55:759–769.
45. Shen X, Gunst SJ, Tepper RS. Effect of tidal volume and frequency on airway responsiveness in mechanically ventilated rabbits. *J Appl Physiol* 1997;83:1202–1208.
46. Mijailovich SM, Fredberg JJ, Butler JP. On the theory of muscle contraction: filament extensibility and the development of isometric force and stiffness. *Biophys J* 1996;71:1475–1484.
47. Nguyen TB, Fredberg JJ. Strange dynamics of a dynamic cytoskeleton. *Proceedings of the American Thoracic Society.* In presss.
48. Trepat X, Deng L, An SS, Navajas D, Tschumperlin DJ, Gerthoffer WT, Butler JP, Fredberg JJ. *Nature* 2007;447:592–595.
49. An SS, Fabry B, Trepat X, Wang N, Fredberg JJ. Do biophysical properties of the airway smooth muscle in culture predict airway hyperresponsiveness? *Am J Respir Cell Mol Biol* 2006;35:55–64.